

Transport of micro-bubbles in turbulent shear flows

This content has been downloaded from IOPscience. Please scroll down to see the full text.

2015 J. Phys.: Conf. Ser. 656 012018

(<http://iopscience.iop.org/1742-6596/656/1/012018>)

View [the table of contents for this issue](#), or go to the [journal homepage](#) for more

Download details:

IP Address: 45.45.132.97

This content was downloaded on 18/09/2016 at 15:37

Please note that [terms and conditions apply](#).

You may also be interested in:

[PIV measurement of a contraction flow using micro-bubble tracer](#)

Masaaki Ishikawa, Kunio Irabu, Isao Teruya et al.

[Flow Structures Around Micro-bubbles During Subcooled Nucleate Boiling](#)

Wang Hao, Peng Xiao-Feng, David M.

Christopher et al.

[Optical and Acoustic Observations of Bubble Adhered to Piezoelectric Transducer under Ultrasound](#)

Field: [Pressure Signal Caused by Bubble Behavior](#)

Shintaro Nakatani, Kenji Yoshida and Yoshiaki Watanabe

[Measurement of micro Bubbles generated by a pressurized dissolution method](#)

S Hosokawa, K Tanaka, A Tomiyama et al.

[Detection of Micro-Bubbles in Thin Polymer Films by Means of Acoustic Resonant Spectroscopy](#)

Hironori Tohyoh and Hidetomo Ikarashi

[Effect of Micro-Bubbles in Water on Beam Patterns of Parametric Array](#)

Kunio Hashiba and Hiroshi Masuzawa

[Some Micro-Disk Patterns on Topaz](#)

A R Patel and K N Goswami

Transport of micro-bubbles in turbulent shear flows

P. Gualtieri, F. Battista and C.M. Casciola

Diaprtimento di Ingegneria Meccanica e Aerospaziale, Sapienza Università di Roma. Via Eudossiana 18, 00184 Roma, Italy

E-mail: paolo.gualtieri@uniroma1.it

Abstract. The dynamics of micro-bubbles, which are typical in many industrial applications, is addressed by means the Direct Numerical Simulations (DNS) of two prototypal flows, namely a homogeneous shear flow and a fully developed pipe flows. This preliminary study has a two-fold purpose. The homogenous turbulent shear flow is useful to characterize the bubble dynamics in terms of their eventual clustering properties which is expected to be controlled by the Stokes number. The time history of the fluid pressure experienced by the bubbles during their evolution is recorded and successively employed to force the Rayleigh-Plesset equation [1]. The ensuing data are used to address *a posteriori* the bubble diameter statistics in view of bubble collapse induced by strong and intermittent turbulent pressure fluctuations. The turbulent pipe flow simulations serve to address the bubble dynamics in wall bounded flows. Here the bubbles are observed to accumulate in the near-wall region with different intensity depending on the bubble dimensions.

1. Introduction

Many natural and technological applications present regimes where micro-bubbles are transported by a carried eventually turbulent flow. For instance, the cavitation events and the collapse of the bubbles are of primary importance in the propeller design due to the structural damages caused by cavitation.

This paper deals with the dynamics of a point-like disperse phase in prototypal turbulent shear flows, a homogeneous shear flow and a pipe flow, laden with *particles* of different density ratios ranging from neutrally buoyant particles with $\rho_p/\rho_f = 1$ to the typical density ratios of the bubbles, i.e. $\rho_p/\rho_f = 10^{-2} - 10^{-3}$. The turbulent carrier flow is resolved by means of the Direct Numerical Simulation of the incompressible Navier-Stokes equations at a moderate value of the Reynolds number. The carrier phase transports inertial particles which are assumed to small in comparison with the smallest hydrodynamical scale, i.e. the Kolmogorov dissipative scale η . In such conditions the particles dynamics is well captured by the equations reported in [2] and [3], namely

$$\frac{d\mathbf{x}_p}{dt} = \mathbf{v}_p(t); \quad \tau_p \frac{d\mathbf{v}_p}{dt} = [\mathbf{u}(\mathbf{x}_p, t) - \mathbf{v}_p(t)] + \frac{3}{2} \frac{\tau_p}{\left(\frac{1}{2} + \frac{\rho_p}{\rho_f}\right)} \frac{D\mathbf{u}}{Dt}(\mathbf{x}_p, t), \quad (1)$$

where \mathbf{x}_p and \mathbf{v}_p are the particle instantaneous position and velocity, respectively, $\mathbf{u}(\mathbf{x}_p, t)$ is the fluid velocity at the particle position, ρ_p/ρ_f is the particle to fluid density ratio,

$\tau_p = (\rho_p/\rho_f)d_p^2/(18\nu_f)$ is the particle relaxation time (with d_p the particle diameter and ν_f the fluid kinematic viscosity). Equations (1) hold for particles whose diameter is smaller than the Kolmogorov scale, $d_p/\eta \ll 1$ and particle Reynolds number smaller than one, $Re_p = (|\mathbf{u} - \mathbf{v}_p|)d_p/\nu_f \ll 1$. The first and second terms on the right hand side of eq. (1) are the Stokes drag and the added mass respectively. In the latter $D\mathbf{u}/Dt$ is the fluid acceleration evaluated at the particle position. Equations (1) are time-integrated following the Lagrangian trajectory of the disperse phase and, when needed, the fluid velocity and the fluid acceleration ensuing from the time-integration of the background turbulent field are interpolated at the particle position.

Panels (a) and (c) of figure 1 address the two geometries considered here, namely the homogeneous shear flow in panel (a) and the turbulent pipe flow in panel (c). Briefly the homogeneous shear flow consists in a 3D periodic box where turbulent fluctuations are forced by an imposed mean velocity gradient see [4]. The computational domain of physical size $4\pi \times 2\pi \times 2\pi$ is discretized by means of $288 \times 144 \times 144$ collocation points where equations are solved by means of a pseudo-spectral method. This allows to resolve the Kolmogorov scale at the selected Reynolds number of $Re_\lambda = 80$. The pipe flow consists in a cylindrical duct with periodic conditions in the axial direction. The motion of the fluid is obtained by enforcing a constant mean pressure gradient along the pipe, see [5]. Here the pipe length is $2\pi R$ where R is the pipe radius. In this case the code exploits staggered finite difference method to solve the Navier-Stokes equations in cylindrical coordinates on a discrete grid of $256 \times 192 \times 256$ points in the azimuthal, radial and axial direction respectively. Both codes take advantage of a low-storage Runge-Kutta scheme for the temporal integration of the carrier and disperse phase.

Several simulations have been performed to span the particle space parameter. In fact, in the limit of small particle Reynolds number $Re_p \ll 1$, the only two parameters describing the different motion regimes of the disperse phase are the particle Stokes number, namely the fluid to particle characteristic time ratio, $St = \tau_p/\tau_f$ and the particle to fluid density ratio ρ_p/ρ_f . Concerning the homogeneous shear flow we have considered three different Stokes numbers, based on the Kolmogorov time scale, and four values of the density ratio, namely $St_\eta = 0.5, 0.1, 0.01$ and $\rho_p/\rho_f = 1, 0.1, 0.01, 0.001$ which amounts to twelve different cases. In the pipe flow two Stokes number, based on the wall-unit time-scale, and five values of the density ratio, namely $St^+ = 0.2, 2$ and $\rho_p/\rho_f = 5, 1, 0.1, 0.01, 0.001$ are available amounting to ten cases. The turbulent Reynolds number based on the Taylor scale is $Re_\lambda = 80$ for the homogeneous shear flow and the friction Reynolds number is $Re_\tau = 310$ for the pipe flow configuration.

2. Results and Discussion

Figure 1 reports the instantaneous configuration of the disperse phase for the two geometries addressed in this paper, namely panel (b) for the homogeneous shear flow and panel (d) for the pipe flow. Some few slices are reported to give a visual representation of the underlying turbulent fluctuations in panels (a) and (c). In the homogeneous shear flow it is shown the instantaneous configuration of the disperse phase pertaining to $St_\eta = 0.5$ and $\rho_p/\rho_f = 0.001$. These are the typical values for bubbles which are well known to accumulate in the low pressure region of the turbulent field, i.e. in the coherent vortical structures. This feature clearly emerge from the scatter plot in panel (b) where the bubbles form filament-like structures which mark to the cores of the turbulent vortices. Concerning the pipe flow, at first sight, no significant spatial localization of particles appears in the case of $St=0.2$ and $\rho_p/\rho_f = 0.001$ probably due to a relatively small value of the Stokes number.

More quantitative statistical results are shown in figure 2. Panels (a) and (b) show the the radial distribution function g_{00} versus the spatial separation r/η . The radial distribution

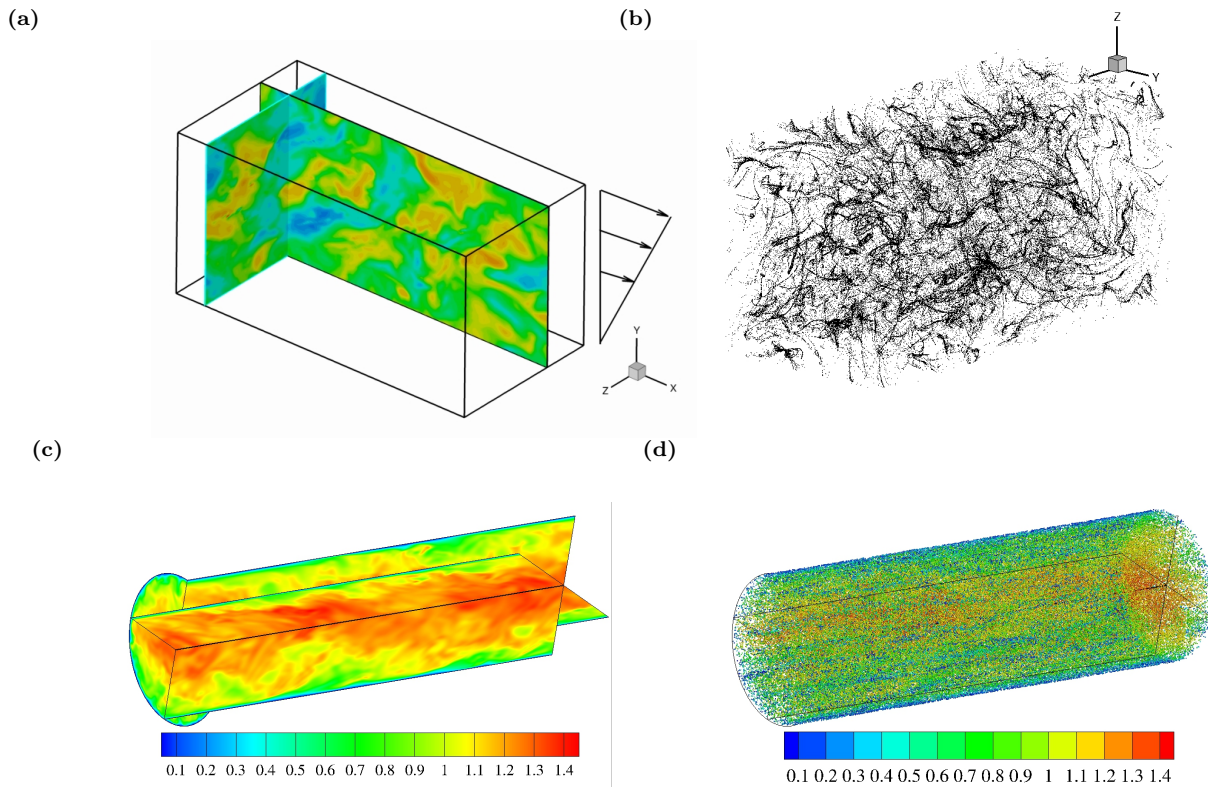


Figure 1. Instantaneous configuration of the fluid domain and for the homogeneous shear flow, panel (a), and for the pipe flow, panel (c). Colors denotes the stream-wise fluid velocity intensity. Panel (b): instantaneous configuration of the disperse phase in the homogeneous shear flow corresponding to $St_\eta = 0.5$ and $\rho_p/\rho_f = 0.001$. Panel (d): instantaneous configuration of the disperse phase in the pipe flow at $St^+ = 0.2$ and $\rho_p/\rho_f = 0.001$. Bubbles are colored with their stream-wise velocity intensity.

function actually measures the probability to find a particle pair at a certain distance r . The different curves in the panel address the effect of the Stokes number St_η at a fixed density ratio $\rho_p/\rho_f = 0.001$ (panel (a)) and the effect of the density ratio at fixed Stokes number $St_\eta = 0.1$ (panel (b)). As expected, for vanishing Stokes number (Lagrangian tracers), the particle distribution behaves as a spatially homogeneous distribution and the radial distribution function assumes the unitary value at all separations. However, when the Stokes number is increased, small scale clustering occurs, i.e. $g_{00}(r)$ diverges at small separations, see figure 2 panel (a). The behavior of particles at fixed Stokes number, $St^+ = 0.1$, depending on the particle/fluid density ratio, shows that for bubbles $\rho_p/\rho_f = 0.001$ the clustering formation is more intense than the other cases $\rho_p/\rho_f \rightarrow 1$. Dealing with the turbulent pipe flow, panels (c) and (d) report the particle mean concentration profile normalized with the homogeneous concentration for two different values of the Stokes number, $St^+ = 2$ panel (c) and $St^+ = 0.5$ panel (d). The disperse phase appears to segregate in the near wall region. In particular the segregation intensity increases with the increase of the Stokes number and the maximum concentration peak moves away from wall by decreasing the particle density, staying in any cases in the viscous sublayer or the buffer layer.

A deeper analysis of the transport of bubbles in a turbulent flow calls into play the particle radius dynamics obtained by the Rayleigh-Plesset [1] forced by the fluid pressure history experienced along their trajectory. In particular, due to the preferential sampling of turbulent

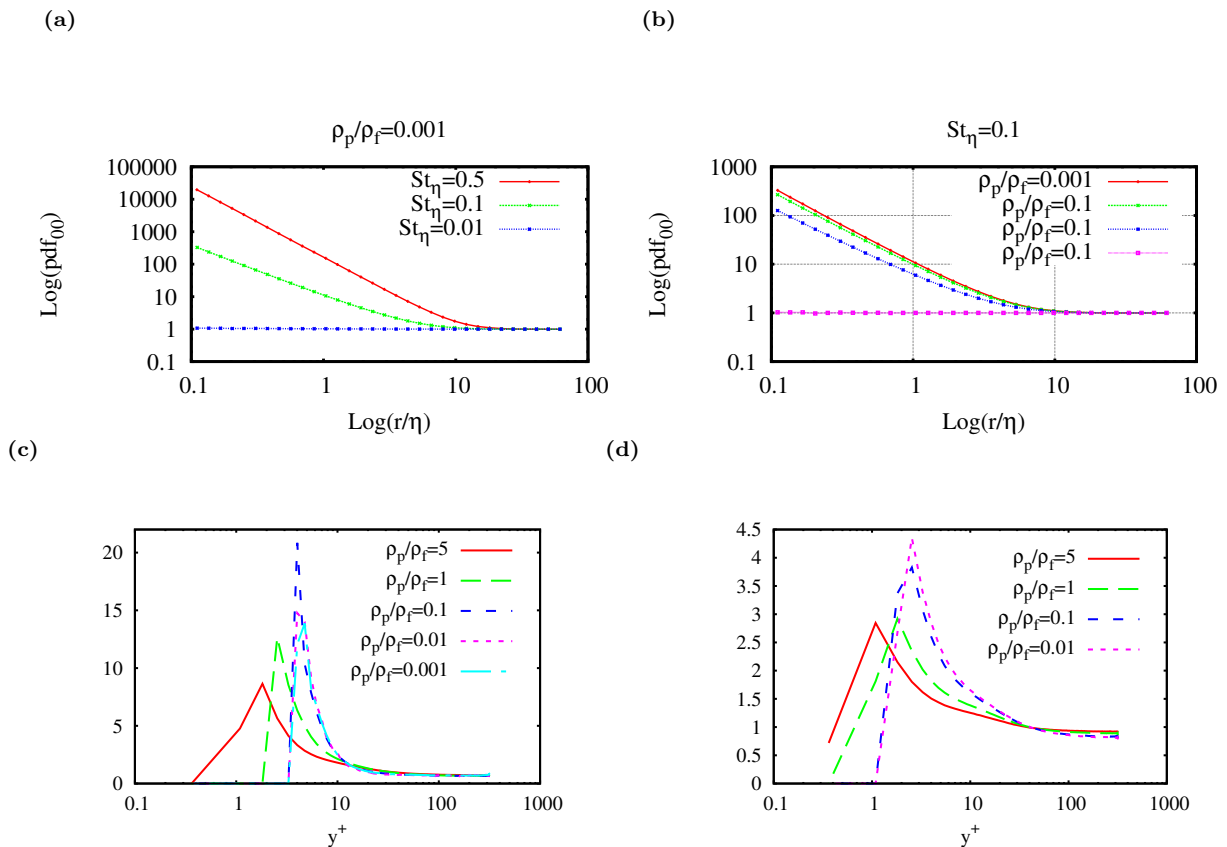


Figure 2. Top panels: radial distribution function g_{00} versus normalized separation r/η at fixed density ratio $\rho_p/\rho_f = 0.001$ and different Stokes number St_η (panel (a)), and at fixed Stokes number $St_\eta = 0.1$ and different density ratios (panel (b)). Bottom panels: wall-normal mean particle concentration as a function of the normalized wall-normal distance $y^+ = (1 - r)/y^*$ where y^* is the wall unit. Two Stokes number are showed, $St^+ = 2$, panel (c), and $St^+ = 0.5$, panel (d).

fluctuations, the light bubbles accumulate in relatively low pressure region of the flow. It follow that the fluctuations of the radius are strongly intermittent and the tails of the ensuing p.d.f is characterized by intense and relatively probable events.

3. Acknowledgments

The present research has received funding from the European Research Council under the European Union's Seventh Framework Program (FP7/ 2007-2013)/ERC Grant Agreement No. [339446]. The authors are grateful to PRACE for awarding access to resource FERMI based in Italy at Casalecchio di Reno

4. References

- [1] Brennen C E 2014 *Cavitation and Bubble Dynamics* (Cambridge University Press)
- [2] Maxey M R and Riley J J 1983 *Physics of Fluids (1958-1988)* **26** 883–889
- [3] Gatignol R 1983 *Journal de Mécanique théorique et appliquée* **2** 143–160
- [4] Gualtieri P, Picano F and Casciola C 2009 *Journal of Fluid Mechanics* **629** 25
- [5] Picano F, Sardina G and Casciola C 2009 *Physics of Fluids* **21** 093305